Precision Higgs at Future Colliders

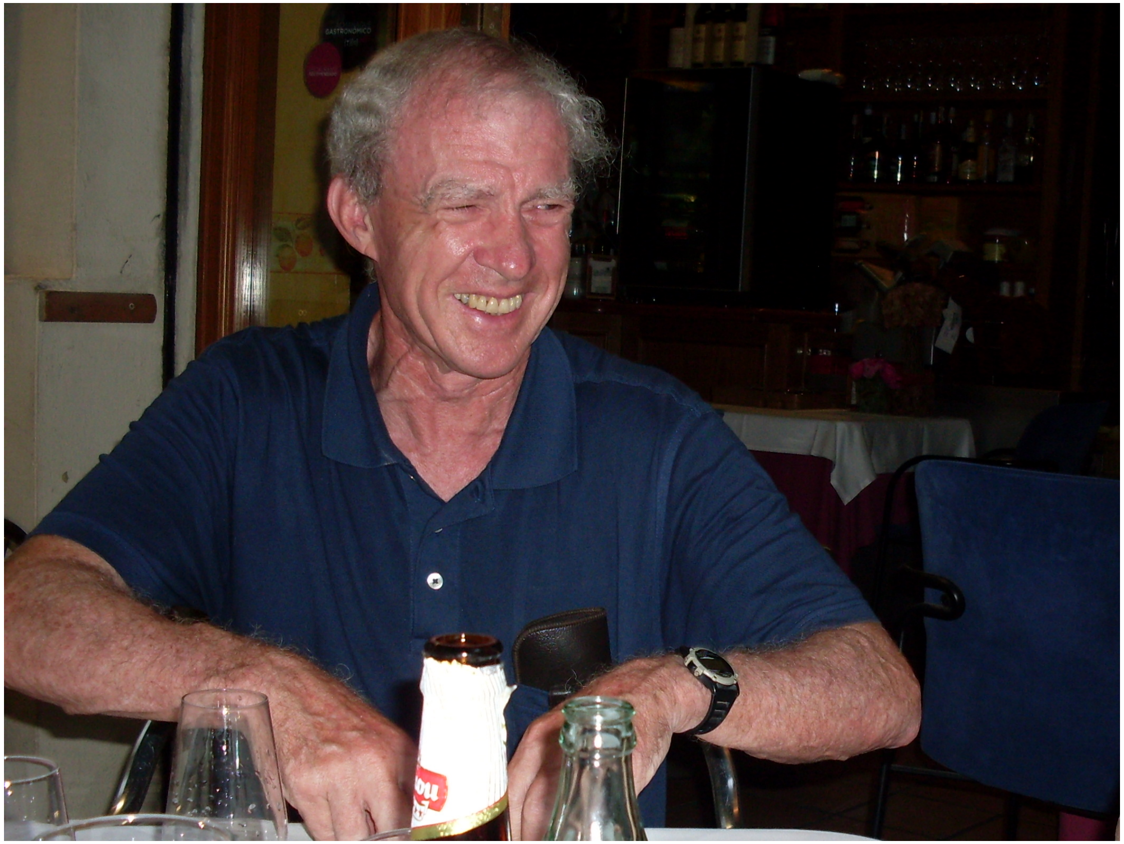

Howard E. Haber
Gunion Fest
UC Davis
March 28, 2014

Timeline of a collaboration

- July, 1978—First meeting at Seattle Summer Institute on the Electroweak Interactions
  - Lost badly at squash
- August, 1981—Second meeting at Seattle Summer Institute on Grand Unification, Supersymmetry and Supergravity
  - Attempt to learn SUSY using four-component spinors (one month before the release of Part 1 of the Supersymmetry Lectures by Wess and Bagger)
  - French feast hosted by three star chef Jean Iliopoulos
- April 21-23, 1983—Fourth Workshop on Grand Unification (FWOGU) held in Philadelphia
  - Jack and I discuss whether it would be useful to provide a comprehensive study of Higgs bosons in the MSSM

Iliopoulos Feast, SUSY-Workshop in Seattle (August, 1981)

It was thirty years ago today…

- My first paper with Jack (and Stan Brodsky), contributed to a workshop on p-bar p options for the supercollider, at Argonne in February, 1984

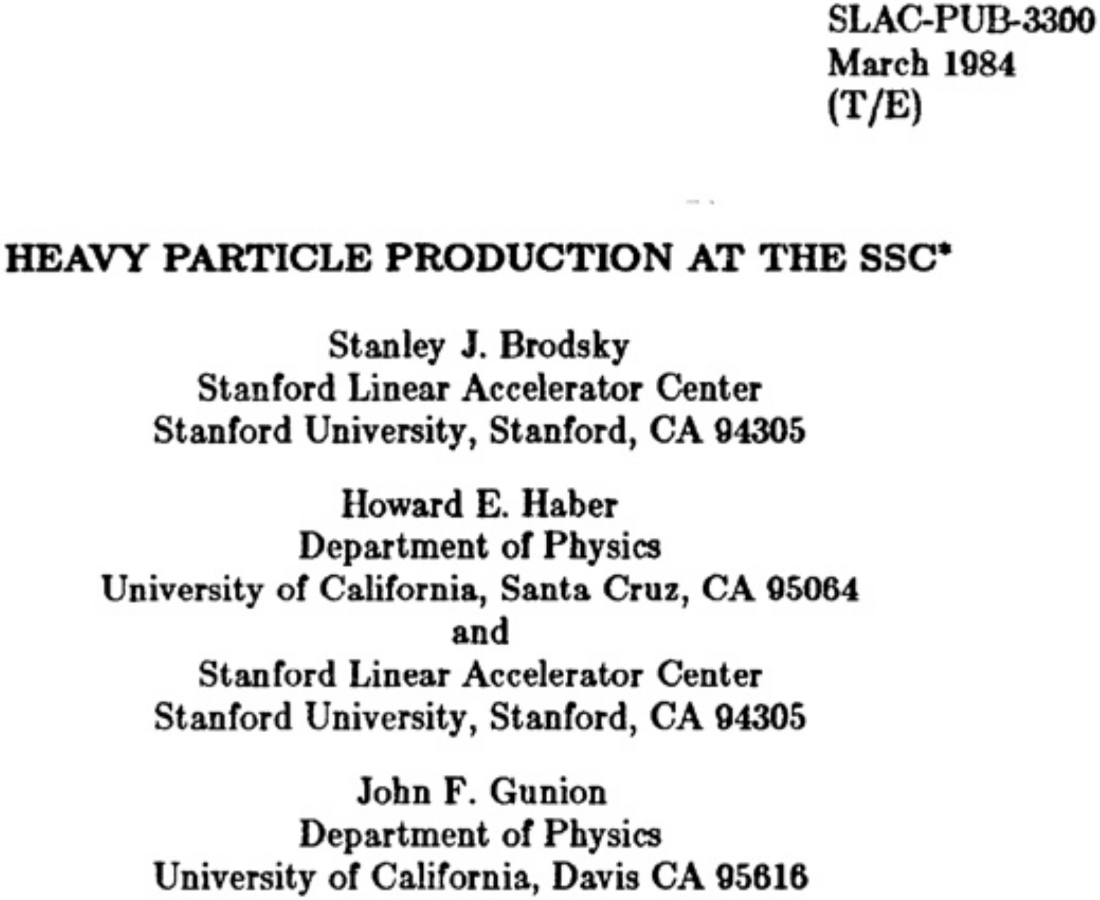

SLAC-PUB-3300
March 1984
(T/E)

HEAVY PARTICLE PRODUCTION AT THE SSC[*]

Stanley J. Brodsky
Stanford Linear Accelerator Center
Stanford University, Stanford, CA 94305

Howard E. Haber
Department of Physics
University of California, Santa Cruz, CA 95064
and
Stanford Linear Accelerator Center
Stanford University, Stanford, CA 94305

John F. Gunion
Department of Physics
University of California, Davis CA 95616

Affectionately called the “intrinsic chevrolet” paper

1984---a seminal year

- June/July, 1984: Snowmass 1984 Workshop
  - Collaboration with Jack on SSC physics takes off

- August, 1984:
  Our paper on Higgs in SUSY is completed.
  - Initially rejected by Nuclear Physics B.
  - After withdrawing the paper, the NPB intervenes and decides to publish.
  - Finally appears on July 14, 1986.
  - Until 2014, remains our most highly cited paper…

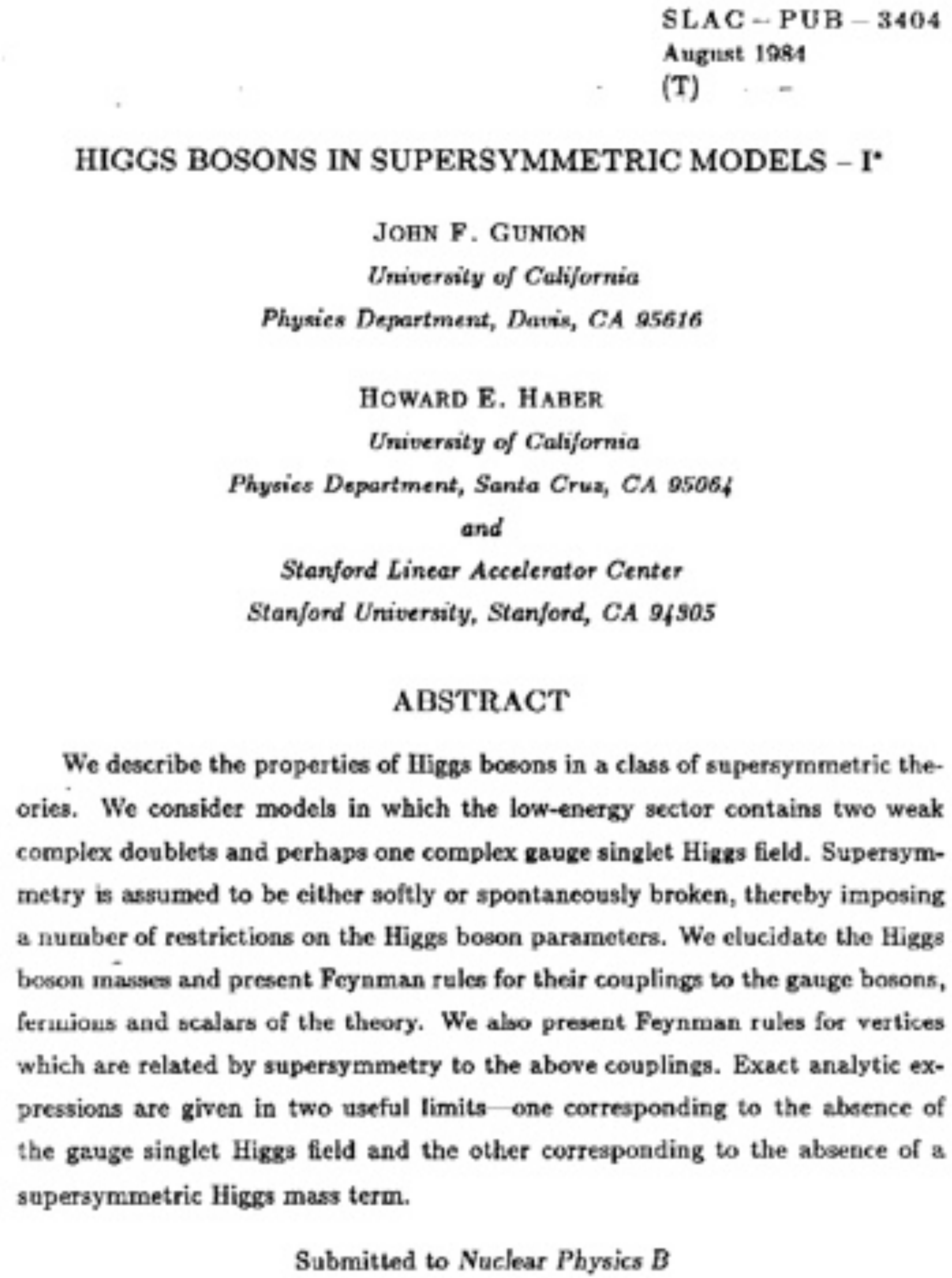

SLAC – PUB – 3404
August 1984
(T)

HIGGS BOSONS IN SUPERSYMMETRIC MODELS – I[*]

JOHN F. GUNION
University of California
Physics Department, Davis, CA 95616

HOWARD E. HABER
University of California
Physics Department, Santa Cruz, CA 95064
and
Stanford Linear Accelerator Center
Stanford University, Stanford, CA 94305

ABSTRACT

We describe the properties of Higgs bosons in a class of supersymmetric theories. We consider models in which the low-energy sector contains two weak complex doublets and perhaps one complex gauge singlet Higgs field. Supersymmetry is assumed to be either softly or spontaneously broken, thereby imposing a number of restrictions on the Higgs boson parameters. We elucidate the Higgs boson masses and present Feynman rules for their couplings to the gauge bosons, fermions and scalars of the theory. We also present Feynman rules for vertices which are related by supersymmetry to the above couplings. Exact analytic expressions are given in two useful limits—one corresponding to the absence of the gauge singlet Higgs field and the other corresponding to the absence of a supersymmetric Higgs mass term.

Submitted to *Nuclear Physics B*

I’m sorry Jack, “Higgs in SUSY 1” just dropped to the Number 2 spot this past week.

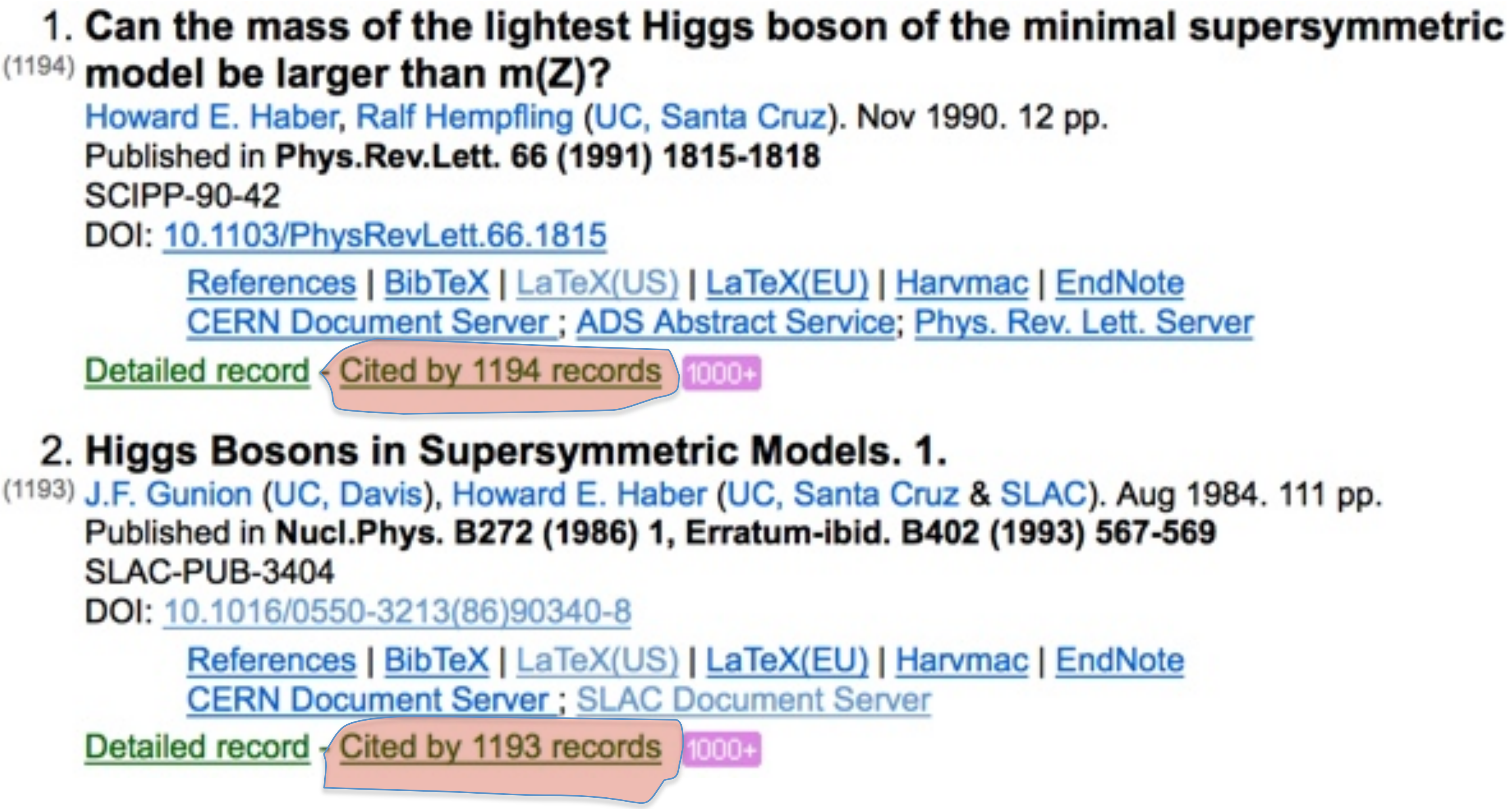

1. **Can the mass of the lightest Higgs boson of the minimal supersymmetric model be larger than m(Z)?**
(1194) Howard E. Haber, Ralf Hempfling (UC, Santa Cruz). Nov 1990. 12 pp.
Published in **Phys.Rev.Lett. 66 (1991) 1815-1818**
SCIPP-90-42
DOI: 10.1103/PhysRevLett.66.1815
References | BibTeX | LaTeX(US) | LaTeX(EU) | Harvmac | EndNote
CERN Document Server ; ADS Abstract Service; Phys. Rev. Lett. Server
Detailed record - Cited by 1194 records 1000+

2. **Higgs Bosons in Supersymmetric Models. 1.**
(1193) J.F. Gunion (UC, Davis), Howard E. Haber (UC, Santa Cruz & SLAC). Aug 1984. 111 pp.
Published in **Nucl.Phys. B272 (1986) 1, Erratum-ibid. B402 (1993) 567-569**
SLAC-PUB-3404
DOI: 10.1016/0550-3213(86)90340-8
References | BibTeX | LaTeX(US) | LaTeX(EU) | Harvmac | EndNote
CERN Document Server ; SLAC Document Server
Detailed record - Cited by 1193 records 1000+

Pursuit of the Higgs boson at future colliders

- 1988—future $e^+ e^-$ colliders: the next generation

- 1989—The Higgs Hunter's Guide

Followed by many enjoyable collaborations over the next 25 years on Higgs, SUSY, BSM physics at SLC and LEP, Tevatron, LHC, and future collider facilities (ILC,…)

FRONTIERS IN PHYSICS

THE HIGGS
HUNTER'S
GUIDE

AIP

John F. Gunion
Howard E. Haber
Gordon Kane
Sally Dawson

30 years later, the collaboration is alive and well

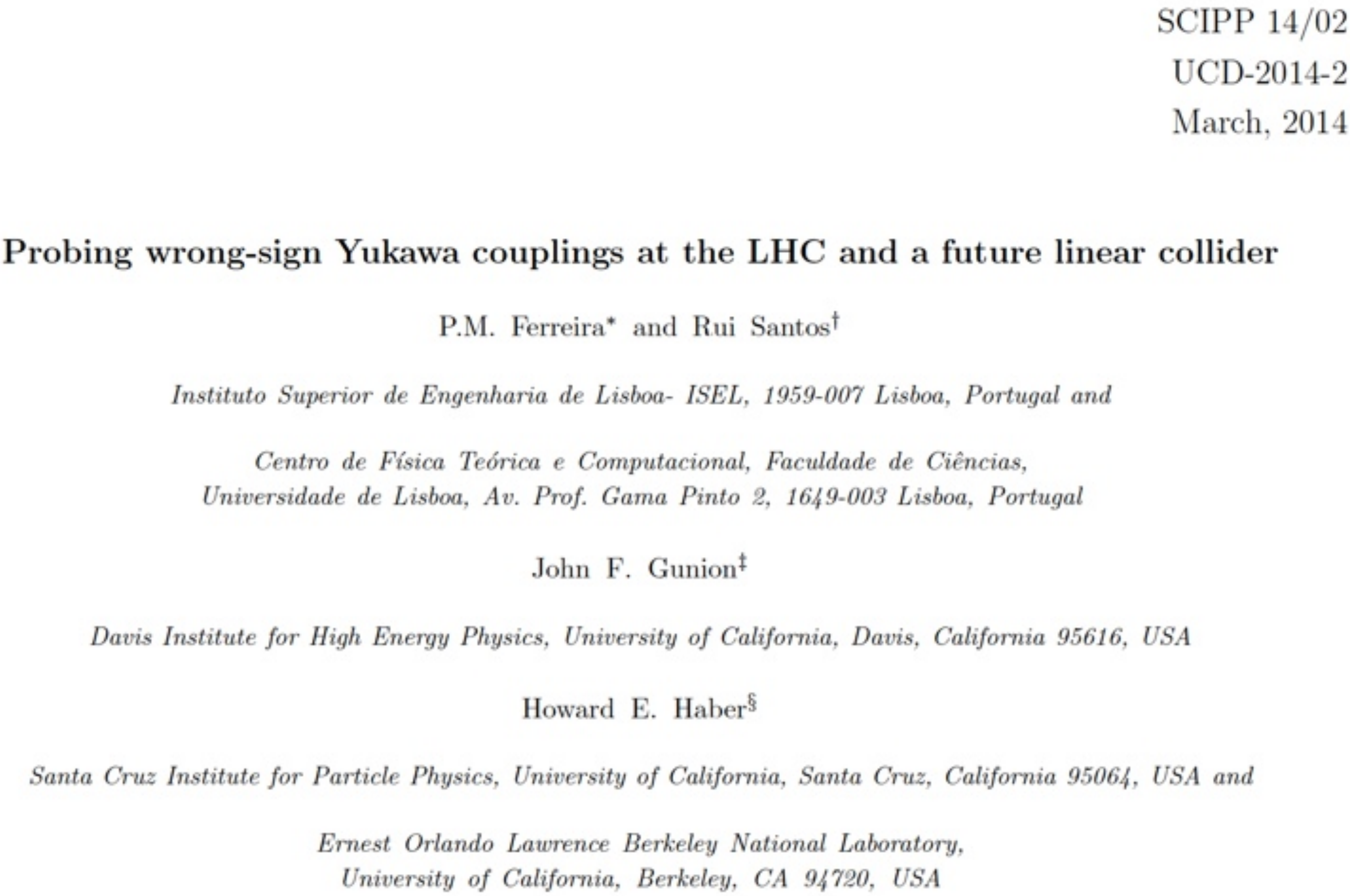

SCIPP 14/02
UCD-2014-2
March, 2014

Probing wrong-sign Yukawa couplings at the LHC and a future linear collider

P.M. Ferreira[*] and Rui Santos[†]

Instituto Superior de Engenharia de Lisboa- ISEL, 1959-007 Lisboa, Portugal and

Centro de Física Teórica e Computacional, Faculdade de Ciências,
Universidade de Lisboa, Av. Prof. Gama Pinto 2, 1649-003 Lisboa, Portugal

John F. Gunion[‡]

Davis Institute for High Energy Physics, University of California, Davis, California 95616, USA

Howard E. Haber[§]

Santa Cruz Institute for Particle Physics, University of California, Santa Cruz, California 95064, USA and

Ernest Orlando Lawrence Berkeley National Laboratory,
University of California, Berkeley, CA 94720, USA

And we are not yet done…

So, at the celebration of your 70th milestone birthday, let me convey my gratitude for your warm friendship and your generosity in sharing your ideas and your dedication to foster this long and fruitful collaboration.

Precision Higgs at Future Colliders

Reference: *ILC Higgs White Paper*,
by D.M. Asner, T. Barklow, C. Calancha,
K. Fujii, N. Graf, H.E. Haber, et al.,
arXiv:1310.0763 [hep-ph], to appear in the
Proceedings of the 2013 Snowmass Community
Study.

See also M.E. Peskin, *Estimation of LHC and ILC Capabilities for Precision Higgs Boson Coupling Measurements*, arXiv:1312.4974 [hep-ph].

ILC : e^+e^- Linear Collider at 250 GeV < $\sqrt{s}$ < 1000 GeV

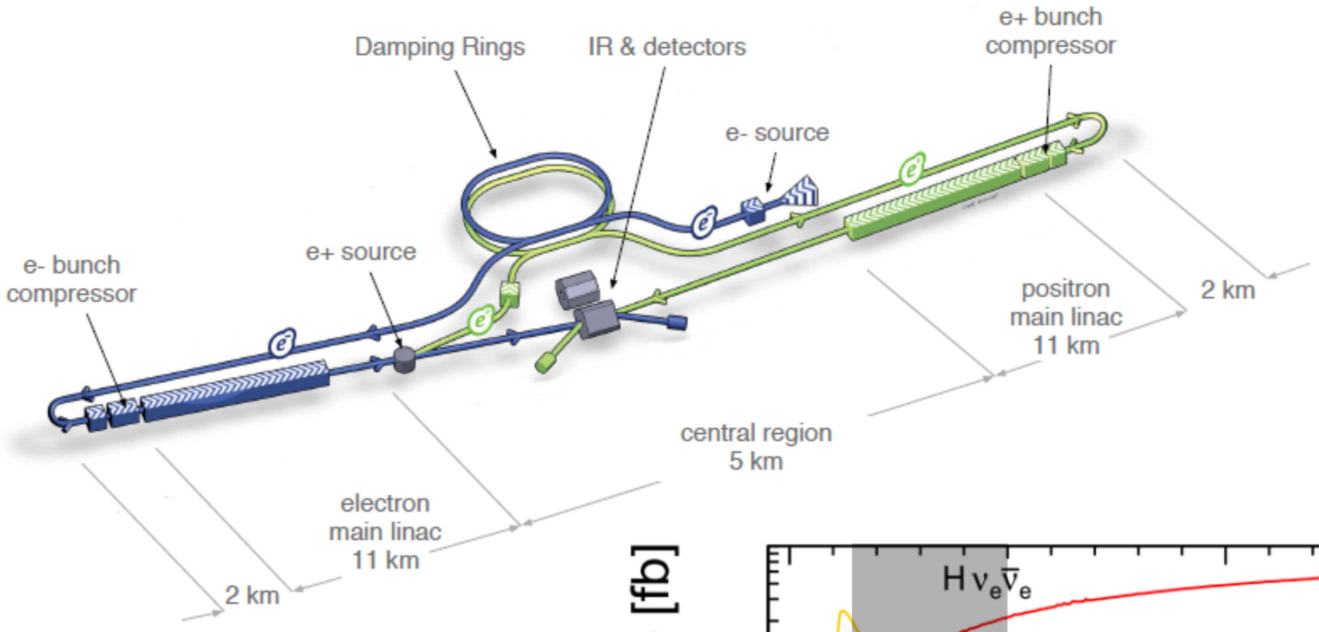

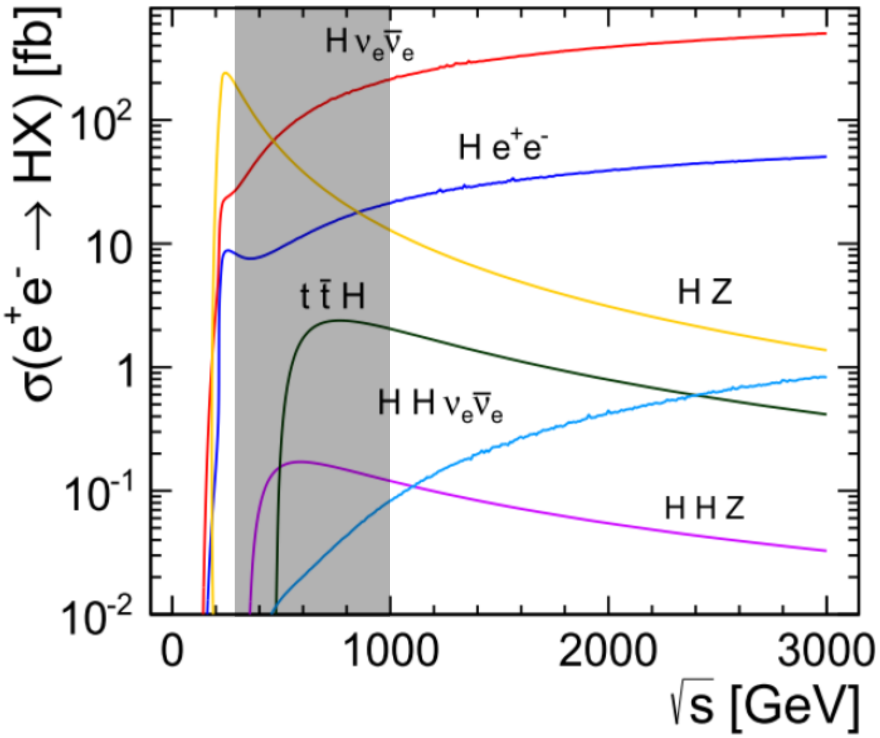

Energy/Luminosity running scenarios

🟧 Baseline Luminosity

🟪 Upgrade Luminosity

From the ILC Technical Design Report

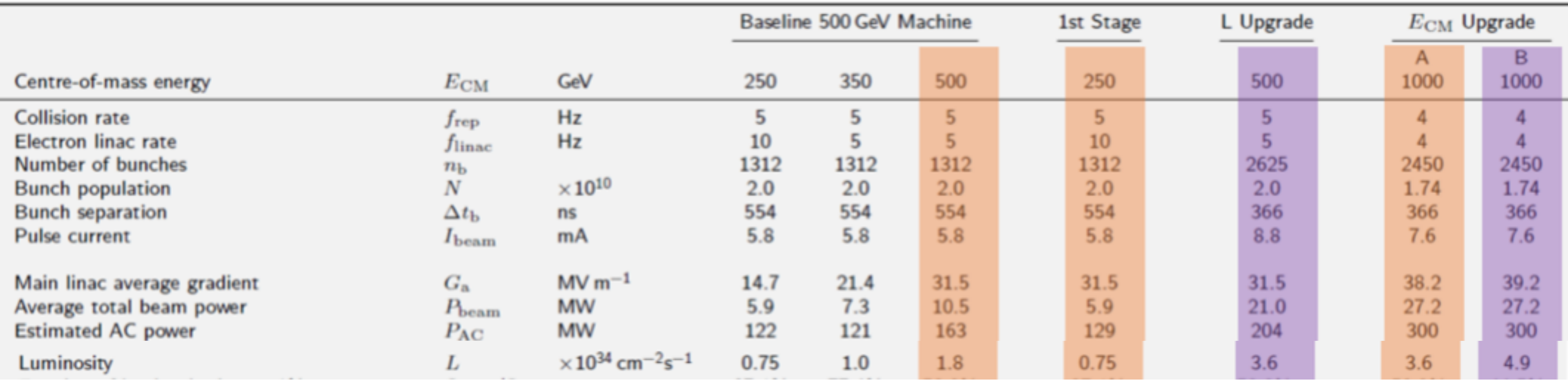

			Baseline 500 GeV Machine			1st Stage	L Upgrade	E_{CM} Upgrade	
								A	B
Centre-of-mass energy	E_{CM}	GeV	250	350	500	250	500	1000	1000
Collision rate	f_{rep}	Hz	5	5	5	5	5	4	4
Electron linac rate	f_{linac}	Hz	10	5	5	10	5	4	4
Number of bunches	n_b		1312	1312	1312	1312	2625	2450	2450
Bunch population	N	$\times 10^{10}$	2.0	2.0	2.0	2.0	2.0	1.74	1.74
Bunch separation	Δt_b	ns	554	554	554	554	366	366	366
Pulse current	I_{beam}	mA	5.8	5.8	5.8	5.8	8.8	7.6	7.6
Main linac average gradient	G_a	MV m^{-1}	14.7	21.4	31.5	31.5	31.5	38.2	39.2
Average total beam power	P_{beam}	MW	5.9	7.3	10.5	5.9	21.0	27.2	27.2
Estimated AC power	P_{AC}	MW	122	121	163	129	204	300	300
Luminosity	L	$\times 10^{34}$ cm^{-2}s^{-1}	0.75	1.0	1.8	0.75	3.6	3.6	4.9

Luminosity (in units of 10^{34} cm^{-2} s^{-1})

CM Energy:	250 GeV	500 GeV	1000 GeV
Baseline design	0.75	1.8	3.6
Luminosity upgrade	3.0*	3.6	4.9

*not in ILC TDR; high rep rate operation proposed by Marc Ross and Nick Walker

Luminosity Upgrade at E_{cm}=250 GeV

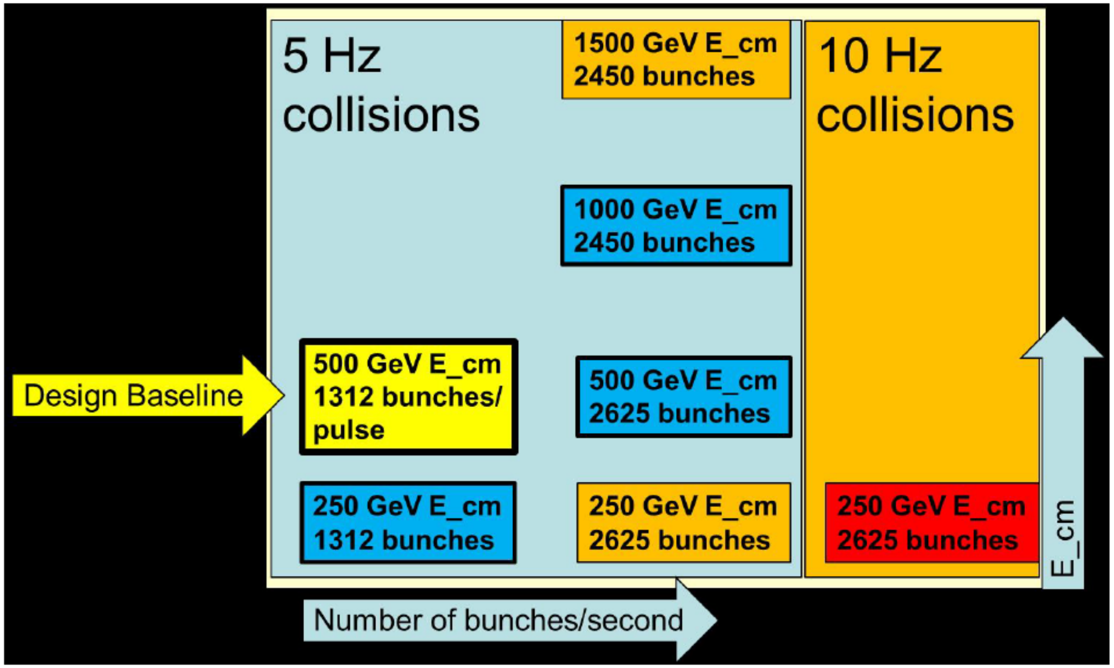

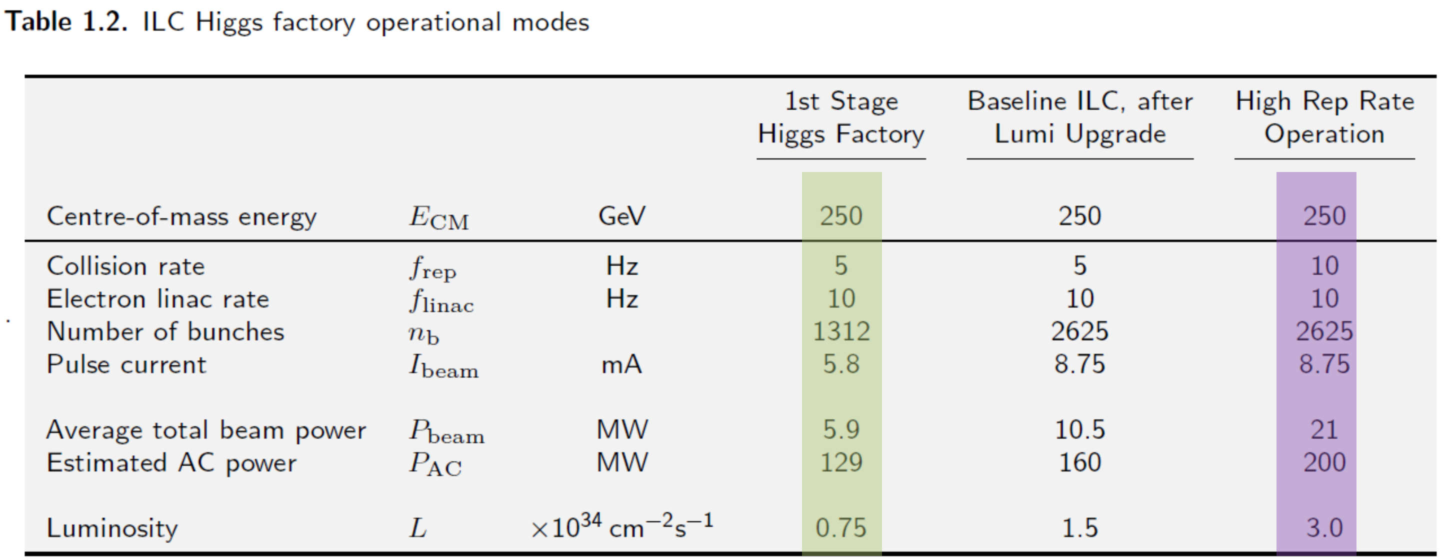

Table 1.2. ILC Higgs factory operational modes

			1st Stage Higgs Factory	Baseline ILC, after Lumi Upgrade	High Rep Rate Operation
Centre-of-mass energy	E_{CM}	GeV	250	250	250
Collision rate	f_{rep}	Hz	5	5	10
Electron linac rate	f_{linac}	Hz	10	10	10
Number of bunches	n_{b}		1312	2625	2625
Pulse current	I_{beam}	mA	5.8	8.75	8.75
Average total beam power	P_{beam}	MW	5.9	10.5	21
Estimated AC power	P_{AC}	MW	129	160	200
Luminosity	L	$\times 10^{34}$ cm^{-2}s^{-1}	0.75	1.5	3.0

🟩 Baseline Luminosity

🟪 Upgrade Luminosity

Energy/Luminosity scenarios

Stage #	nickname	E_{cm}(1) (GeV)	Lumi (1) (fb^{-1})	E_{cm}(2) (GeV)	Lumi (2) (fb^{-1})	E_{cm}(3) (GeV)	Lumi (3) (fb^{-1})	Runtime (years)
1	ILC (250)	250	250					1.1
2	ILC (500)	250	250	500	500			2.0
3	ILC (1000)	250	250	500	500	1000	1000	2.9
4	ILC(LumUp)	250	1150	500	1600	1000	2500	5.8

- At each stage, the *accumulated* luminosity of a given energy is listed. The runtimes listed consist of actual elapsed *cumulative* running time at the end of each stage. Assuming that the ILC runs for 1/3 of the time, then the actual time elapsed is equal to the runtime times 3.

- Assume that the ILC is run at its baseline luminosity at 250 GeV (stage 1), then at 500 GeV (stage 2), and finally at 1000 GeV (stage 3)

- Then, stage 4 repeats the successive stages 1, 2 and 3 at the upgraded luminosity.

In real time, this entire program would require 5.8 x 3 = 17.4 years.

Beam polarization can increase the vector boson fusion cross section, $W^+W^- \rightarrow H$, by as much as a factor of two.

P(e⁻,e⁺)=(0,0)

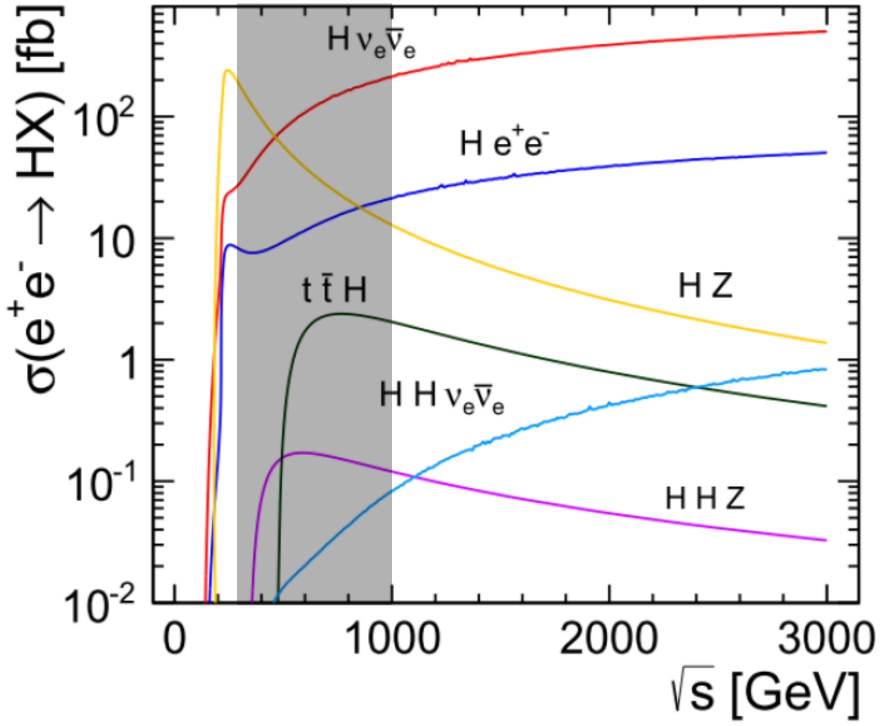

P(e⁻, e⁺)=(-0.8, 0.2)

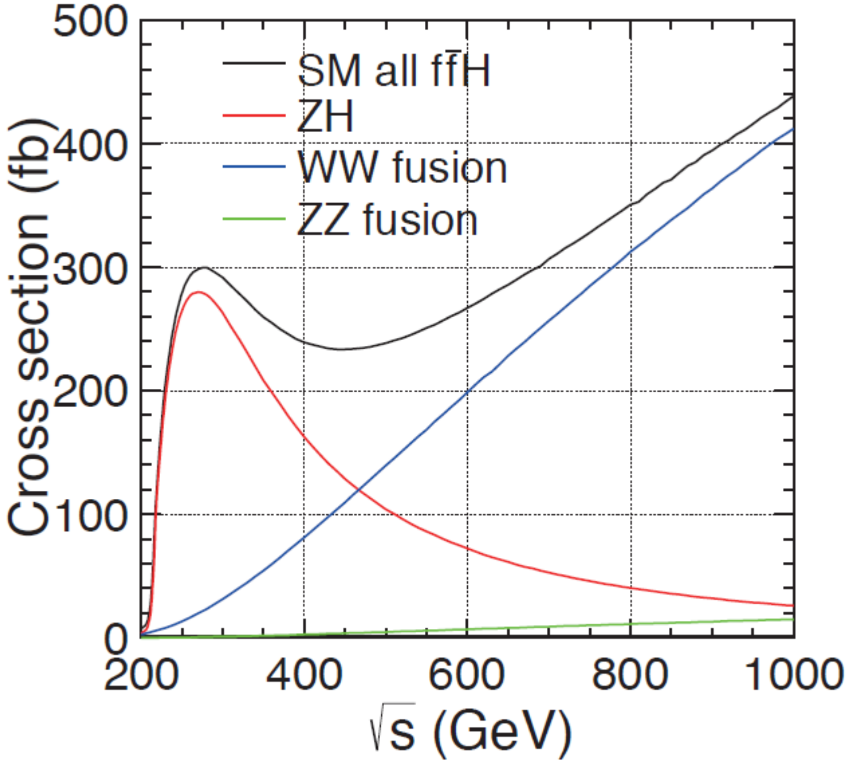

Simulations: Full simulations performed with ILD and/or SiD dectector.

Systematic errors:

	Baseline	LumiUP
luminosity	0.1%	0.05%
polarization	0.1%	0.05%
b-tag efficiency	0.3%	0.15%

What does the ILC actually measure?

1. $\sigma(e^+e^- \to ZH)$ at $\sqrt{s} = 250\ \mathrm{GeV}.$

- The *Z* can be reconstructed in charged lepton and quark channels.
- The *H* can be "seen" in the mass spectrum recoiling against the *Z* (including the invisible Higgs decays).
- The *H* can be reconstructed in its main decay channels.

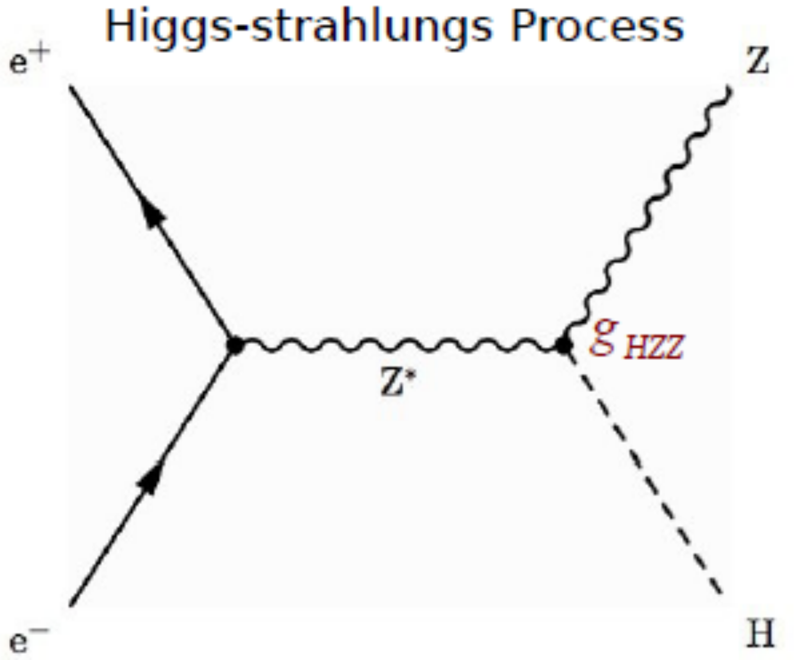

Invisible Higgs Decay

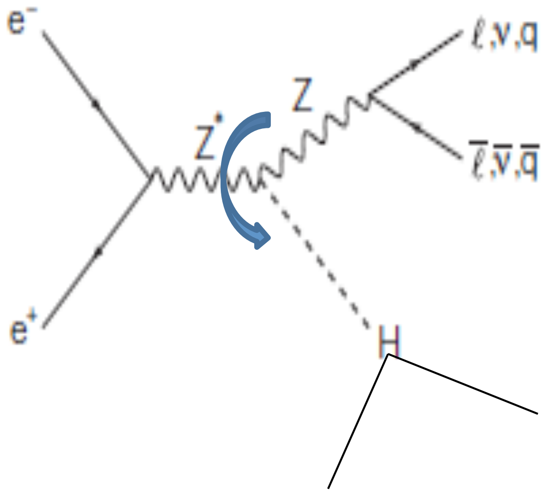

- In the SM, an invisible Higgs decay is H → ZZ* →4ν process and its BF is small ~0.1%
- If we found sizable invisible Higgs decays, it is clear new physics signal.
  - The decay products are dark matter candidates.

- At the LHC, one can search for invisible Higgs decays by using recoil mass from Z or summing up BFs of observed decay modes with some assumptions.
  - The upper limit is O(10%).
- At the ILC, we can search for invisible Higgs decays using a recoil mass technique with model independent way!
  - e+e- → ZH

$$P_H = \underset{\substack{\uparrow \\ \text{known}}}{P_{e+e-}} - \underset{\substack{\uparrow \\ \text{measured}}}{P_Z}$$

$e^+e^- \to ZH,\ \ Z \to \mathrm{qq},\ \ \mathrm{H} \to \mathrm{invisible} \qquad \sqrt{s} = 250\ \mathrm{GeV}$

Signal+Background

Polarizations P(e+,e-)=(+30%,-80) [denoted below as "Left"]
=(-30%, +80%) [denoted below as "Right"]

- If BF(H→invisible) = 3%
  - Signal is clearly seen for "Right" polarization

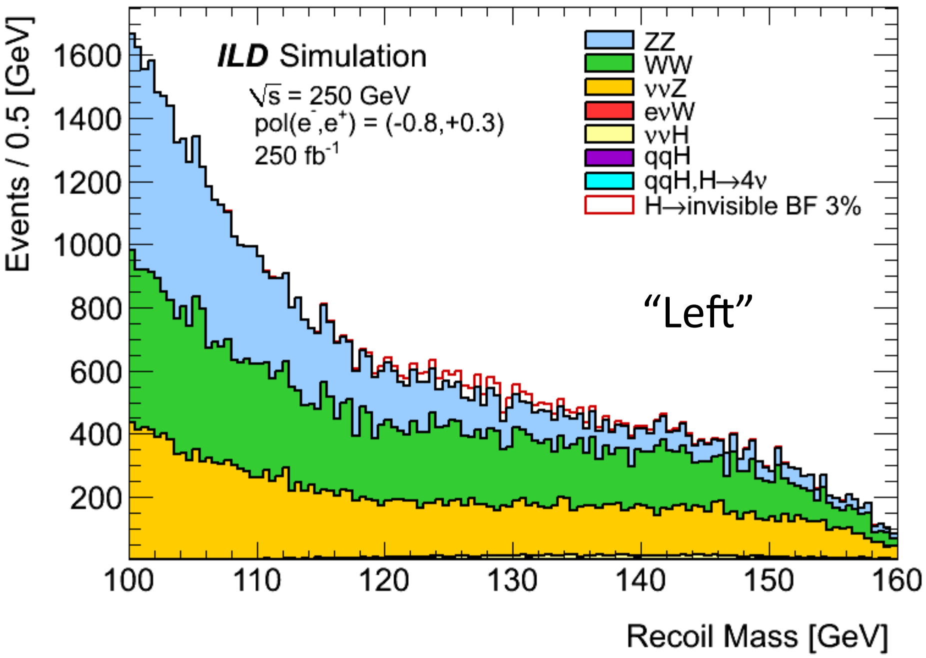

"Left"

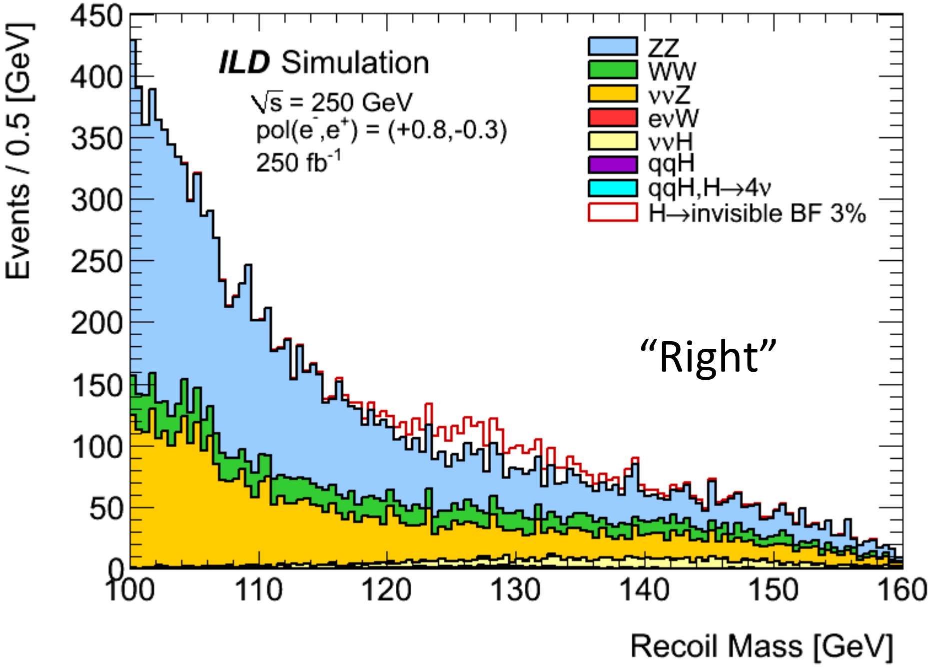

"Right"

2. By explicitly reconstructing H, one obtains

$$\sigma_{ZH} \times \mathrm{Br}(H \to XX)$$

for $XX = b\bar{b}$, $c\bar{c}$, gg, WW^*, $\tau^+\tau^-$, ZZ^*, $\gamma\gamma$ and $\mu^+\mu^-$. Strictly speaking g stands for a hadron jet not identified as a b or c quark. For a SM-like Higgs boson, the Higgs decay into gg dominates over the decays into $u\bar{u}$, $d\bar{d}$ and $s\bar{s}$. (Likewise, Higgs decay into e^+e^- is assumed to be negligible.)

3. Since the ZH production cross section dominates the cross section for $e^+e^- \to \nu\bar{\nu}W^+W^- \to \nu\bar{\nu}H$ at $\sqrt{s} = 250$ GeV, one can only measure $\sigma_{\nu\bar{\nu}H} \times \mathrm{Br}(H \to b\bar{b})$.

4. $e^+e^- \to \nu\bar{\nu}H$, $t\bar{t}H$ and ZHH at $\sqrt{s} = 500$ GeV

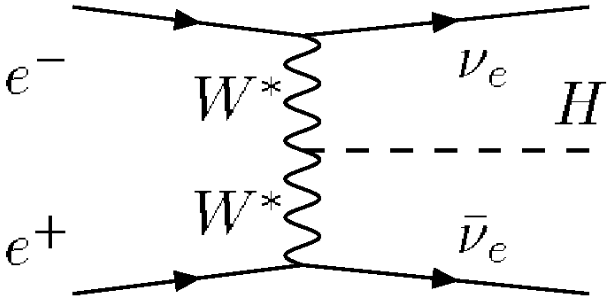

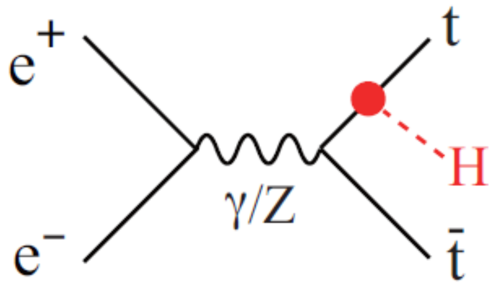

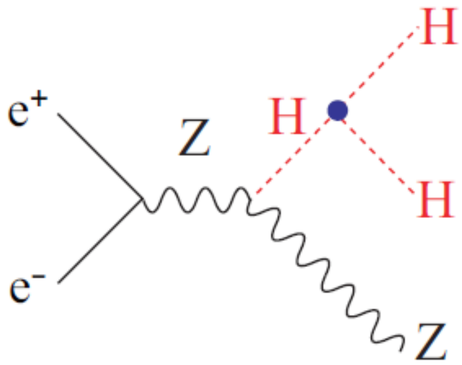

- The WW fusion cross section is now competitive with the ZH cross section. Thus, one can now measure

$$\sigma_{\nu\bar{\nu}H} \times \mathrm{Br}(H \to XX)\,,$$

for all the relevant Higgs channels.

- The cross section for $e^+e^- \to t\bar{t}H$ is enhanced near threshold, and yields a measurement of $\sigma_{t\bar{t}H} \times \mathrm{Br}(H \to b\bar{b})$. From this, one can determine the top quark–Higgs Yukawa coupling.

- The process $e^+e^- \to ZHH$ is sensitive to the HHH coupling, although there are other diagrams contributing to ZHH production that do not depend on the triple Higgs vertex.

5. $e^+e^- \to \nu\bar{\nu}H$, $t\bar{t}H$ and $\nu\bar{\nu}HH$ at $\sqrt{s} = 1$ TeV

At $\sqrt{s} = 1$ TeV, the ILC provides better measurements of the top quark Yukawa coupling and the triple Higgs coupling. Moreover, the Higgs production rate has increased significantly from its rate at $\sqrt{s} = 500$ GeV due to the increasing WW fusion cross section.

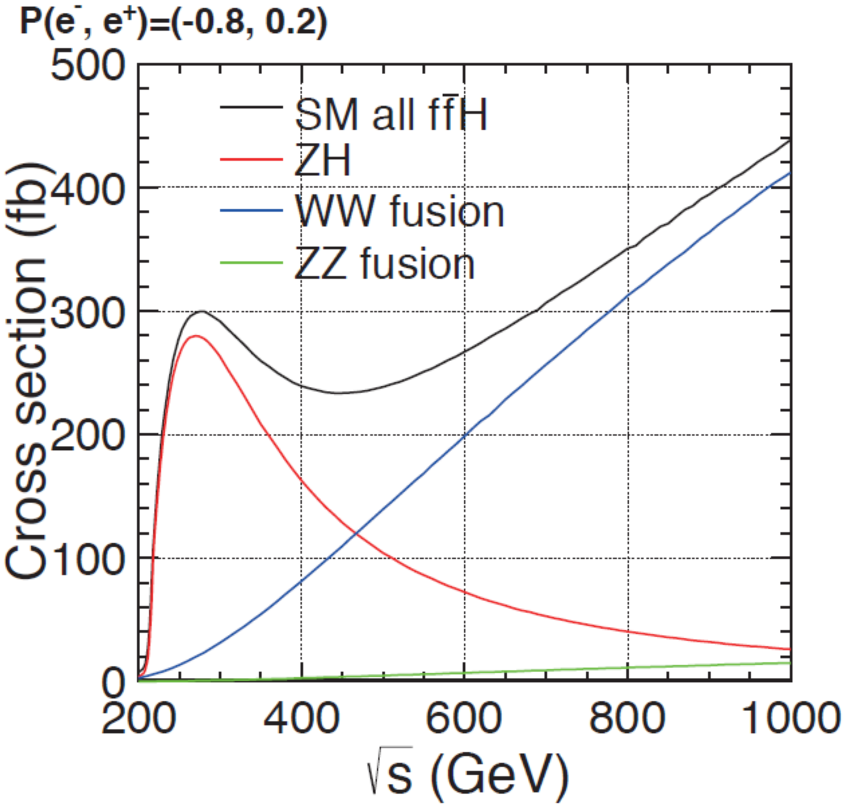

Expected precision for cross section and cross section times branching ratio at the baseline luminosity and a one year runtime (i.e. three years in real time) for each energy/luminosity

$\sqrt{s}$ and $\mathcal{L}$ (P_{e^-}, P_{e^+})	$250\,\mathrm{fb}^{-1}$ at $250\,\mathrm{GeV}$ $(-0.8,+0.3)$		$500\,\mathrm{fb}^{-1}$ at $500\,\mathrm{GeV}$ $(-0.8,+0.3)$				$1\,\mathrm{ab}^{-1}$ at $1\,\mathrm{TeV}$ $(-0.8,+0.2)$		
	Zh	$\nu\bar{\nu}h$	Zh	$\nu\bar{\nu}h$	$t\bar{t}h$	Zhh	$\nu\bar{\nu}h$	$t\bar{t}h$	$\nu\bar{\nu}hh$
$\Delta\sigma/\sigma$	2.6%	-	3.0	-		42.7%			26.3%
BR(invis.)	< 0.9 %	-	-	-	-				
mode	$\Delta(\sigma \cdot BR)/(\sigma \cdot BR)$								
$h \to b\bar{b}$	1.2%	10.5%	1.8%	0.7%	28%		0.5%	6.0%	
$h \to c\bar{c}$	8.3%	-	13%	6.2%			3.1%		
$h \to gg$	7.0%	-	11%	4.1%			2.3%		
$h \to WW^*$	6.4%	-	9.2%	2.4%			1.6%		
$h \to \tau^+\tau^-$	4.2%	-	5.4%	9.0%			3.1%		
$h \to ZZ^*$	19%	-	25%	8.2%			4.1%		
$h \to \gamma\gamma$	34%	-	34%	23%			8.5%		
$h \to \mu^+\mu^-$	100%	-	-	-			31%		

For invisible decays, the 95% CL upper limit is given.
Note: Mass measurement at E_{CM}=250 GeV yields ΔM_H=32 MeV.

Expected accuracies for cross section and cross section times branching ratio at the upgraded luminosity and a one year runtime (i.e. three years in real time) for each energy/luminosity

$\sqrt{s}$ and $\mathcal{L}$ (P_{e^-}, P_{e^+})	$1150\,\mathrm{fb}^{-1}$ at $250\,\mathrm{GeV}$ $(-0.8,+0.3)$		$1600\,\mathrm{fb}^{-1}$ at $500\,\mathrm{GeV}$ $(-0.8,+0.3)$				$2.5\,\mathrm{ab}^{-1}$ at $1\,\mathrm{TeV}$ $(-0.8,+0.2)$		
	Zh	$\nu\bar{\nu}h$	Zh	$\nu\bar{\nu}h$	$t\bar{t}h$	Zhh	$\nu\bar{\nu}h$	$t\bar{t}h$	$\nu\bar{\nu}hh$
$\Delta\sigma/\sigma$	1.2%	-	1.7	-		23.7%			16.7%
BR(invis.)	< 0.4 %	-	-	-			-		
mode	$\Delta(\sigma \cdot BR)/(\sigma \cdot BR)$								
$h \to b\bar{b}$	0.6%	4.9%	1.0%	0.4%	16%		0.3%	3.8%	
$h \to c\bar{c}$	3.9%	-	7.2%	3.5%			2.0%		
$h \to gg$	3.3%	-	6.0%	2.3%			1.4%		
$h \to WW^*$	3.0%	-	5.1%	1.3%			1.0%		
$h \to \tau^+\tau^-$	2.0%	-	3.0%	5.0%			2.0%		
$h \to ZZ^*$	8.8%	-	14%	4.6%			2.6%		
$h \to \gamma\gamma$	16%	-	19%	13%			5.4%		
$h \to \mu^+\mu^-$	46.6%	-	-	-			20%		

For invisible decays, the 95% CL upper limit is given.
Note: Mass measurement at E_{CM}=250 GeV yields ΔM_H=15 MeV.

Model-independent determinations of Higgs couplings

Example--consider the following four independent measurements:

$$Y_1 = \sigma_{ZH} = F_1 \cdot g^2_{HZZ}$$

$$Y_2 = \sigma_{ZH} \times \mathrm{Br}(H \to b\bar{b}) = F_2 \cdot \frac{g^2_{HZZ} g^2_{Hb\bar{b}}}{\Gamma_T}$$

$$Y_3 = \sigma_{\nu\bar{\nu}H} \times \mathrm{Br}(H \to b\bar{b}) = F_3 \cdot \frac{g^2_{HWW} g^2_{Hb\bar{b}}}{\Gamma_T}$$

$$Y_4 = \sigma_{\nu\bar{\nu}H} \times \mathrm{Br}(H \to WW^*) = F_4 \cdot \frac{g^4_{HWW}}{\Gamma_T}$$

Γ_T is the Higgs total width, g_{HZZ}, g_{HWW}, and $g_{Hb\bar{b}}$ are the Higgs couplings to ZZ, WW, and $b\bar{b}$, respectively, and F_1, F_2, F_3, F_4 are calculable quantities. For example,

$$F_2 = \left(\frac{\sigma_{ZH}}{g^2_{HZZ}}\right)\left(\frac{\Gamma_{H\to b\bar{b}}}{g^2_{Hb\bar{b}}}\right) \, .$$

The couplings are obtained as follows:

1. From $Y_1 \quad \Longleftrightarrow \quad g_{HZZ}$
2. From $Y_1 Y_3/Y_2 \quad \Longleftrightarrow \quad g_{HWW}$
3. From g_{HWW} and $Y_4 \quad \Longleftrightarrow \quad \Gamma_T$
4. From g_{HZZ}, g_{HWW}, Γ_T and Y_2 or $Y_3 \quad \Longleftrightarrow \quad g_{Hb\bar{b}}$

We perform a global fit for the Higgs couplings and Γ_T using σ_{ZH} and the 33 $\sigma \times$ Br's listed in the previous tables. Each observable Y_i can be written formally as

$$Y_i = Y_i'(F_i, g_{HXX}, \Gamma_T)\,,$$

where g_{HXX} runs over the various possible Higgs couplings. The F_i are theoretical quantities with some error. We expect that $\Delta F_i = 0.5\%$ is a reasonable assumption at the time of ILC running (some suggest that errors as low as 0.1% are achievable).

Let $(\Delta Y_i)^2$ be the sum in quadrature of the error on the measurement Y_i and the total theory error for Y_i'. We obtain the g_{HXX} by minimizing the chi-square function,

$$\chi^2 = \sum_i \left(\frac{Y_i - Y_i'}{\Delta Y_i}\right)^2\,.$$

Summary of expected accuracies $\Delta g_i/g_i$ and Γ_T for model independent determinations of the Higgs boson couplings

Mode	ILC(250)	ILC(500)	ILC(1000)	ILC(LumUp)
$\sqrt{s}$ (GeV)	250	250+500	250+500+1000	250+500+1000
L (fb^{-1})	250	250+500	250+500+1000	1150+1600+2500
$\gamma\gamma$	18 %	8.4 %	4.0 %	2.4 %
gg	6.4 %	2.3 %	1.6 %	0.9 %
WW	4.9 %	1.2 %	1.1 %	0.6 %
ZZ	1.3 %	1.0 %	1.0 %	0.5 %
$t\bar{t}$	–	14 %	3.2 %	2.0 %
$b\bar{b}$	5.3 %	1.7 %	1.3 %	0.8 %
$\tau^+\tau^-$	5.8 %	2.4 %	1.8 %	1.0 %
$c\bar{c}$	6.8 %	2.8 %	1.8 %	1.1 %
$\mu^+\mu^-$	91 %	91 %	16 %	10 %
Γ_T	12 %	5.0 %	4.6 %	2.5 %
hhh	–	83 %	21 %	13 %
BR(invis.)	< 0.9 %	< 0.9 %	< 0.9 %	< 0.4 %

The theory errors are $\Delta F_i/F_i$=0.5%. For the invisible branching ratio, the numbers quoted are 95% confidence upper limits.

Model-independent determinations of Higgs cross sections and branching ratios

We choose the fit parameters to be three cross sections, σ_{ZH}, $\sigma_{\nu\bar{\nu}H}$, $\sigma_{t\bar{t}H}$, and eight branching ratios, $\mathrm{Br}(H \to b\bar{b})$, $\mathrm{Br}(H \to c\bar{c})$, $\mathrm{Br}(H \to gg)$, $\mathrm{Br}(H \to WW^*)$, $\mathrm{Br}(H \to ZZ^*)$, $\mathrm{Br}(H \to \tau^+\tau^-)$, $\mathrm{Br}(H \to \mu^+\mu^-)$, $\mathrm{Br}(H \to \gamma\gamma)$.

For example, in the ILC(1000) luminosity scenario we use the measured cross-section σ_{ZH}, the 33 independent $\sigma \times \mathrm{Br}$ measurements and the appropriately redefined Y_i' functions to solve for the 11 fit parameters through the minimization of an alternate χ^2 function.

Summary of expected accuracies for the three cross sections and eight branching ratios obtained from an eleven parameter global fit of all available data.

	ILC(250)	ILC500	ILC(1000)	ILC(LumUp)
process	$\Delta\sigma/\sigma$			
$e^+e^- \to ZH$	2.6 %	2.0 %	2.0 %	1.0 %
$e^+e^- \to \nu\bar{\nu}H$	11 %	2.3 %	2.2 %	1.1 %
$e^+e^- \to t\bar{t}H$	-	28 %	6.3 %	3.8 %
mode	ΔBr/Br			
$H \to ZZ$	19 %	7.5 %	4.2 %	2.4 %
$H \to WW$	6.9 %	3.1 %	2.5 %	1.3 %
$H \to b\bar{b}$	2.9 %	2.2 %	2.2 %	1.1 %
$H \to c\bar{c}$	8.7 %	5.1 %	3.4 %	1.9 %
$H \to gg$	7.5 %	4.0 %	2.9 %	1.6 %
$H \to \tau^+\tau^-$	4.9 %	3.7 %	3.0 %	1.6 %
$H \to \gamma\gamma$	34 %	17 %	7.9 %	4.7 %
$H \to \mu^+\mu^-$	100 %	100 %	31 %	20 %

The LHC Timeline

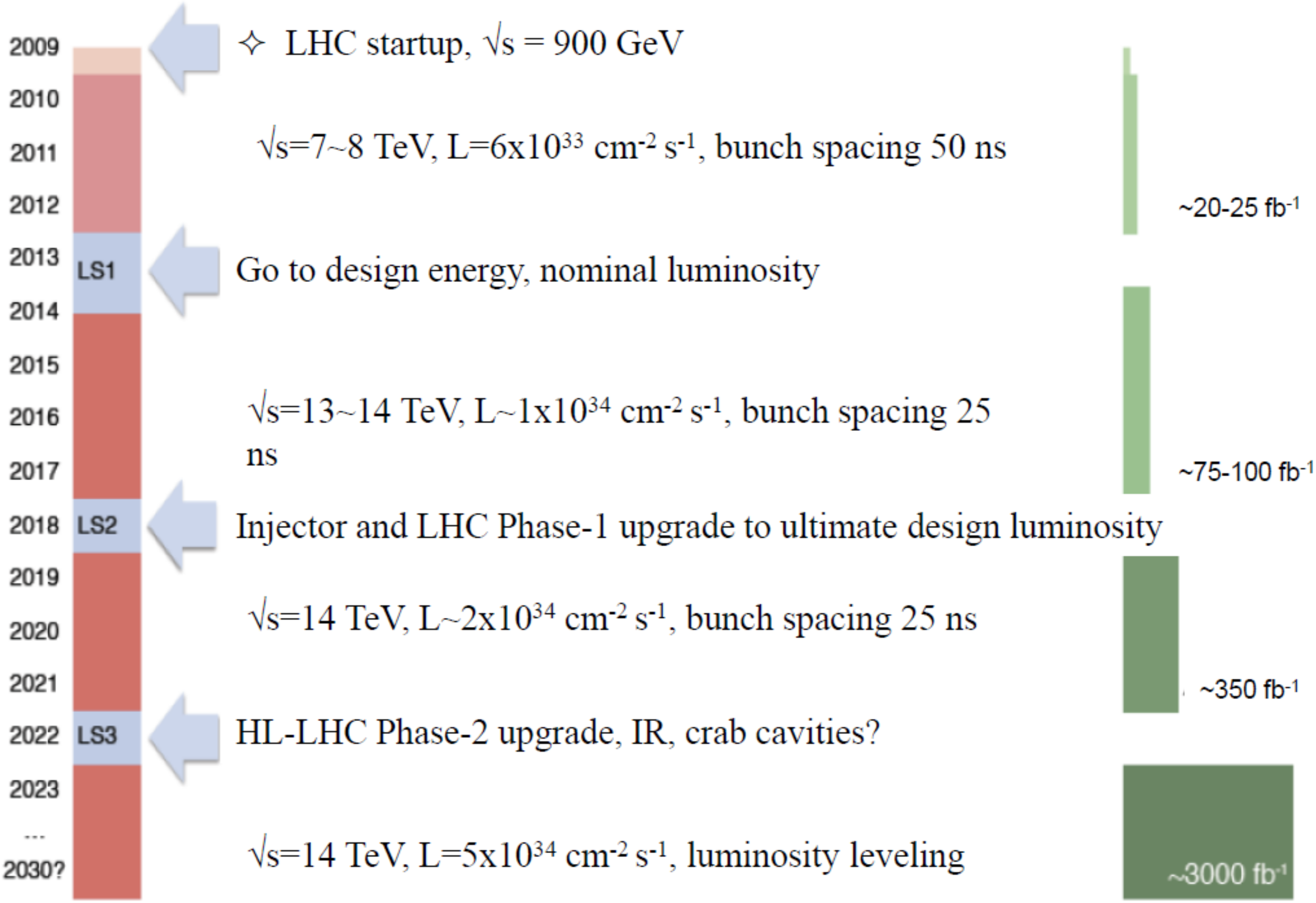

✧ LHC startup, $\sqrt{s} = 900$ GeV

$\sqrt{s}$=7~8 TeV, L=6x10^{33} cm^{-2} s^{-1}, bunch spacing 50 ns

Go to design energy, nominal luminosity

$\sqrt{s}$=13~14 TeV, L~1x10^{34} cm^{-2} s^{-1}, bunch spacing 25 ns

Injector and LHC Phase-1 upgrade to ultimate design luminosity

$\sqrt{s}$=14 TeV, L~2x10^{34} cm^{-2} s^{-1}, bunch spacing 25 ns

HL-LHC Phase-2 upgrade, IR, crab cavities?

$\sqrt{s}$=14 TeV, L=5x10^{34} cm^{-2} s^{-1}, luminosity leveling

Comparing LHC and ILC Projected Precision

ATLAS and CMS have provided projections for the ultimate accuracies of Higgs coupling measurements based on the currently planned six year program (accumulating 300 fb^{-1} of data) and a proposed high-luminosity ten year program (accumulating 3000 fb^{-1} of data).

Here, I make use of Michael Peskin's reinterpretation of the CMS results, which are less conservative than the ATLAS numbers. Since ATLAS does not provide projections for the measurement of the hbb coupling, Peskin only employs the CMS numbers in his analysis.

CMS quotes a pessimistic and optimistic scenario:

CMS-1: current systematic and theoretical uncertainties
are employed.

CMS-2: theoretical errors are reduced by a factor of two
and systematic errors are assumed to decrease
as the square root of the integrated luminosity.

In comparing with ILC precision estimates, Peskin improves the ILC Higgs White paper numbers by imposing the constraint:

$$\sum_i \mathrm{BR}_i = 1$$

based on anticipated measured upper limits for BR’s of exotic Higgs decay modes.

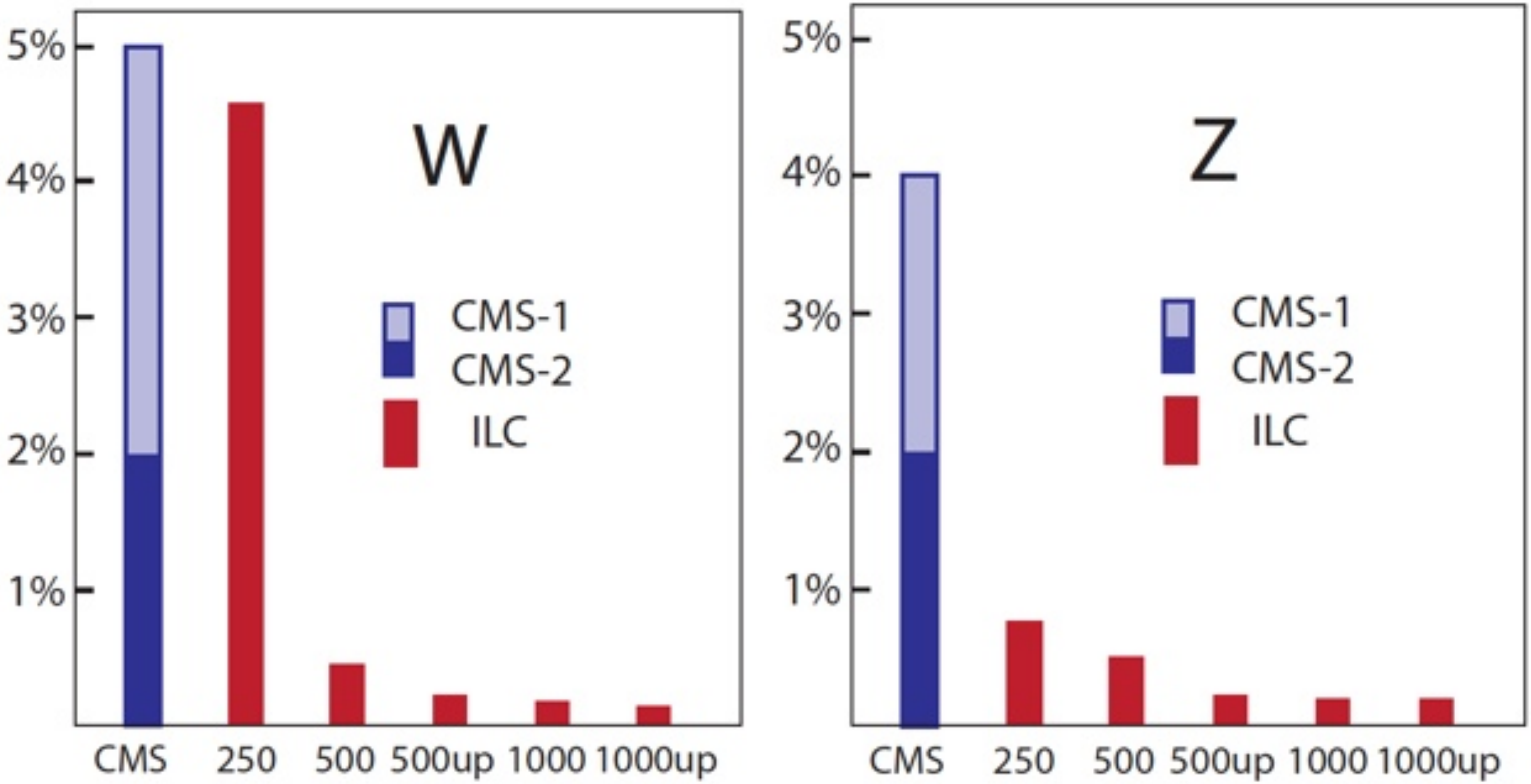

Figure 1: Estimates of the ILC measurement accuracies for the Higgs boson couplings to WW and ZZ. These estimates are based on the 10-parameter fit described in the text. The successive entries correspond to the stages of the ILC program shown in Table 4. The CMS Scenario 1 and Scenario 2 estimates for 3000 fb^{-1}, from [7], are shown on the left.

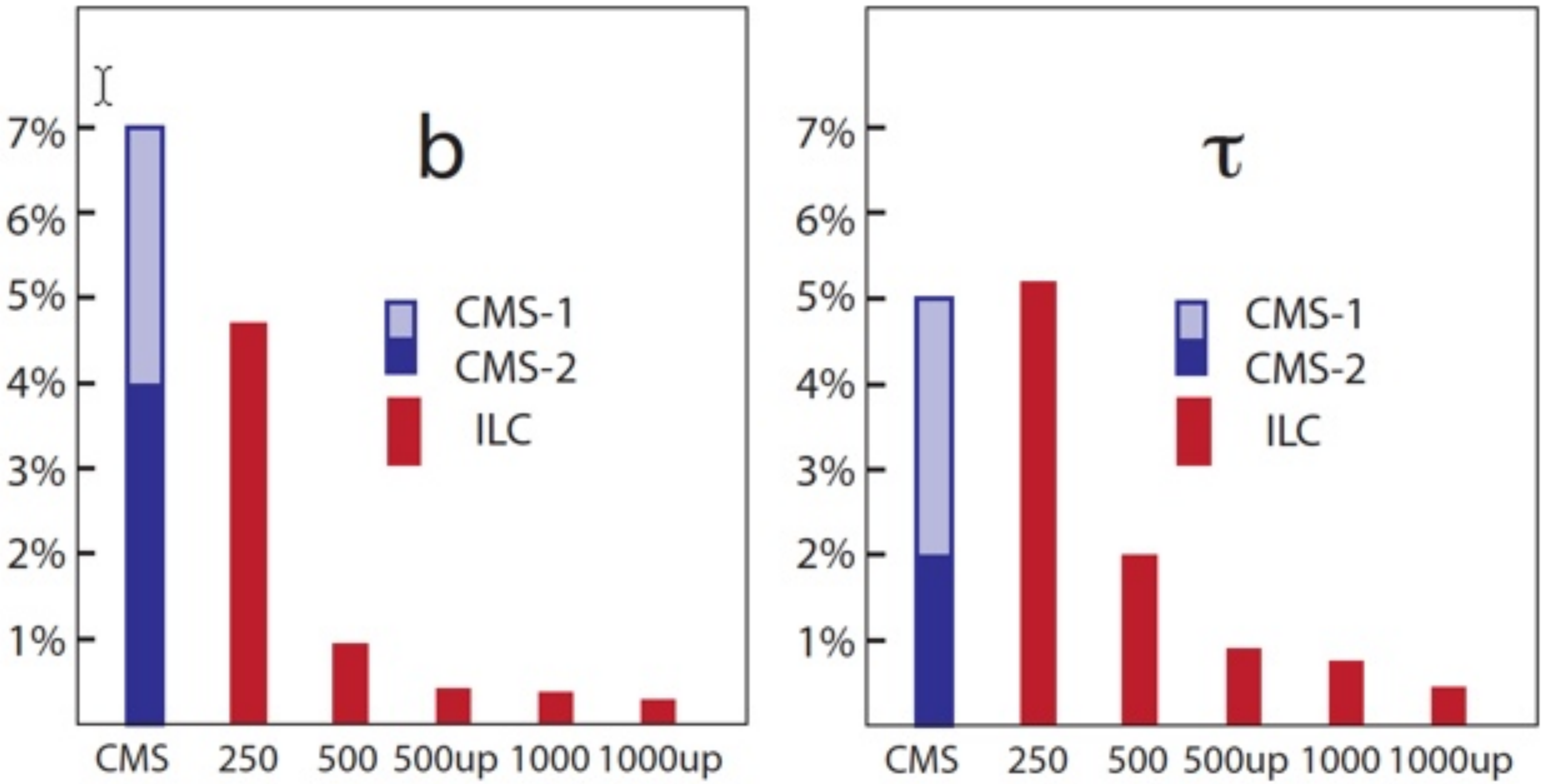

Figure 2: Estimates of the ILC measurement accuracies for the Higgs boson couplings to $b\bar{b}$ and $\tau^+\tau^-$. These estimates are based on the 10-parameter fit described in the text. The successive entries correspond to the stages of the ILC program shown in Table [4]. The CMS Scenario 1 and Scenario 2 estimates for 3000 fb^{-1}, from [7], are shown on the left.

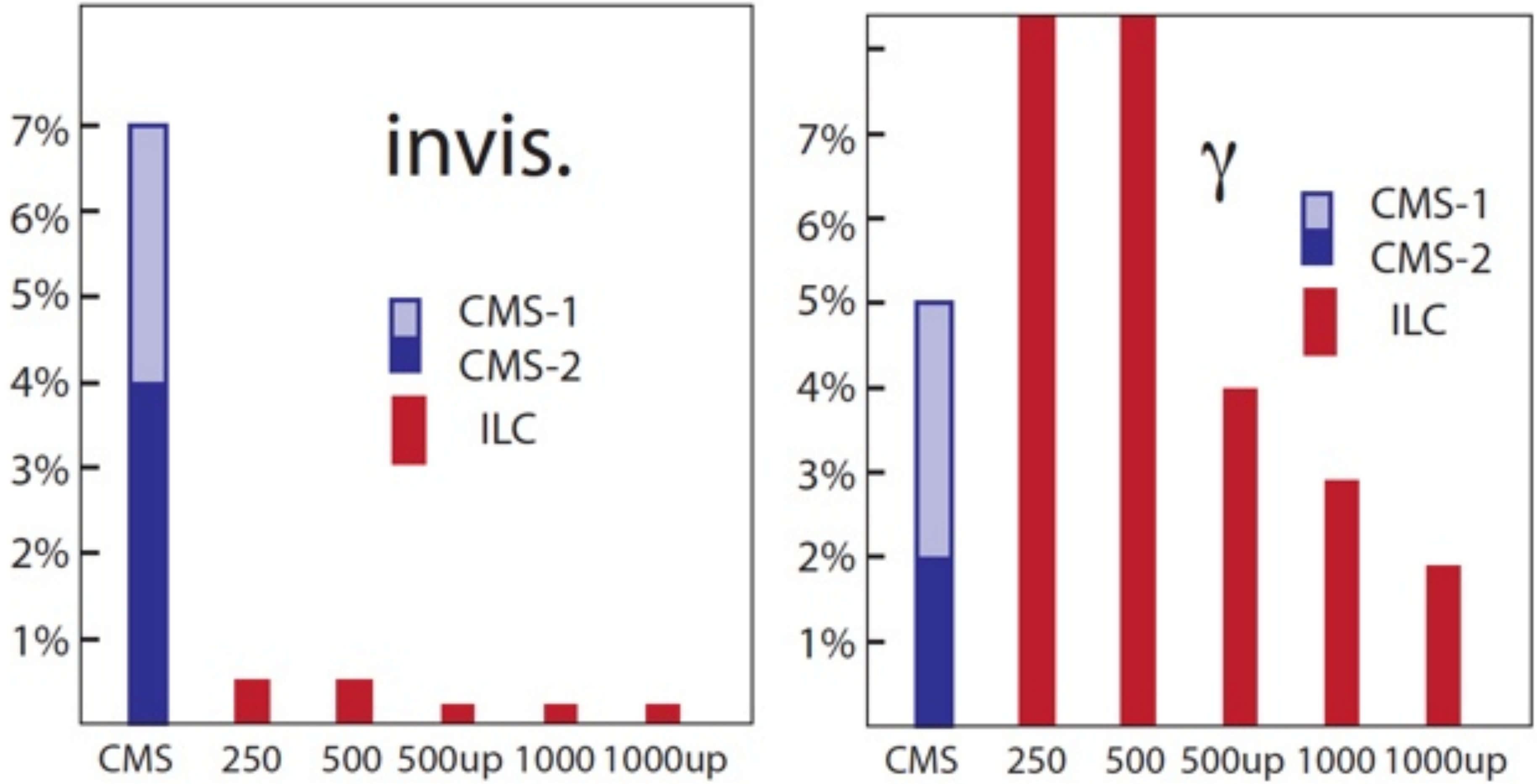

Figure 3: Estimates of the ILC measurement accuracies for the Higgs boson couplings to invisible modes and to $\gamma\gamma$. These estimates are based on the 10-parameter fit described in the text. The successive entries correspond to the stages of the ILC program shown in Table 4. The CMS Scenario 1 and Scenario 2 estimates for 3000 fb^{-1}, from [7], are shown on the left.

Peskin notes that by combining one LHC observable, namely

$$\Delta \frac{\mathrm{BR}(H \to \gamma\gamma)}{\mathrm{BR}(H \to ZZ^*)} = 3.6\%$$

as projected by ATLAS in their high luminosity LHC analysis, with the ILC precision measurement of the *ZZH* coupling, one is able to obtain a very precise determination of the γγ*H* coupling.

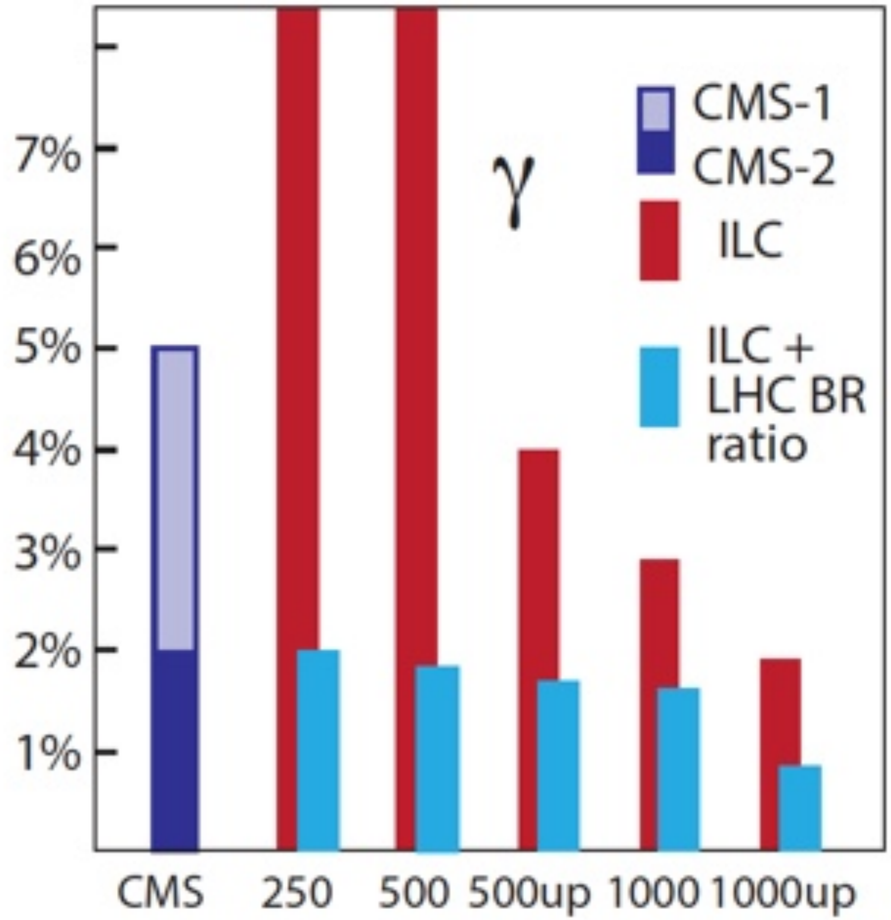

Figure 4: Estimates of the ILC measurement accuracies for the Higgs boson couplings to $\gamma\gamma$ when combined with the measurement of $BR(\gamma\gamma)/BR(ZZ^*)$ projected by ATLAS [6]. The successive entries correspond to the stages of the ILC program shown in Table 4. The CMS Scenario 1 and Scenario 2 estimates for 3000 fb^{-1}, from [7], are shown on the left.

The Bottom Line

- The ILC will provide the next significant step in the precision study of Higgs boson properties. LHC precision measurements in the 5—10% range will be brought down to the 1% level.

- The ILC is able to provide a model-independent determination of Higgs couplings via the measurement of σ_{ZH}, in addition to measuring σ x Br in numerous channels. (In contrast, LHC only can measure σ x Br).

- Together with the LHC Higgs data, the ILC will provide critical measurements that can probe new physics beyond the Standard Model and provide important clues as to what may lie ahead.